2021

In vivo analysis of lysyl oxidase deletion in mice, a pilot study

BOSTON UNIVERSITY

HENRY M. GOLDMAN SCHOOL OF DENTAL MEDICINE

THESIS

IN VIVO ANALYSIS OF LYSYL OXIDASE DELETION IN MICE, A PILOT STUDY

by

TYLER JAMES GUINN

B.S., Grand Valley State University, 2014
DDS, University of Michigan, 2018

Submitted in partial fulfillment of the requirements for the degree of

Master of Science in Dentistry
In the Department of Translational Dental Medicine

2021

Approved by:

First Reader _____

Dr. Philip C. Trackman, Ph.D.
Emeritus Professor of Translational Dental Medicine

Second Reader _____

Dr. Manish Bais, Ph.D.
Associate Professor of Translational Dental Medicine

DEDICATION

I would like to dedicate this work to my parents Jim and MaryBeth, my brother Tony, and lastly to my wonderful wife, AJ.

ACKNOWLEDGMENTS

Vrinda Dambal for her work with the histological analysis and submission of μCT specimens for imaging.

Dr. Philip C. Trackman for all his tireless efforts in my pursuit of this Masters thesis.

Center for skeletal research imaging and biomechanical testing Core NIH P30 AR070542 for their imaging and statistical analysis of the specimens submitted.

IN VIVO ANALYSIS OF LYSYL OXIDASE DELETION IN MICE, A PILOT STUDY

TYLER JAMES GUINN

Boston University, Henry M. Goldman School of Dental Medicine, 2021

Major Professor: Dr. Philip C. Trackman, Ph.D.
Emeritus Professor of Translational Dental Medicine

ABSTRACT

Lysyl Oxidase (LOX) is a key enzyme for the production of collagen cross-links in connective tissue development. This study investigated the phenotypic effects of mouse *Lox* deletion using Cre-recombinase technology driven by the promoter of the osteoblast specific hormone osteocalcin. 6 Female *Ocn-cre*-/-, *Lox* $^{fl/fl}$; 6 female *Ocn-cre*$^{+/-}$, *Lox*$^{fl/fl}$; 6 male *Ocn-cre*$^{-/-}$, *Lox*$^{fl/fl}$, and 6 male *Ocn-cre*$^{+/-}$, *Lox*$^{fl/fl}$ were sacrificed at 13-weeks for µCT and histological analysis. µCT data revealed statistically significant reduction in Bone Volume/Total Volume (BV/TV) (P<.003), Connective Tissue Density (ConnD) (P<.012), Bone Mineral Density (BMD) (P<.001), and Structural Model Index (SMI) (P<.004). Male 13-week old *Ocn-cre*$^{+/-}$, *Lox*$^{fl/fl}$ mice showed no statistically significant differences in any parameters analyzed. Histological analysis showed decreases in the number of chondrocytes per column in the *cre*$^{+/-}$ female and male mice. The largest differences in number of chondrocytes per column were found in female *cre*$^{+/-}$ mice. Thus, osteoblast specific knockout of *Lox* appeared to show phenotypic affects more strongly in females rather than male mice. Further analysis into *Lox* knockout should be conducted.

TABLE OF CONTENTS

LIST OF FIGURES

INTRODUCTION

Lysyl Oxidase (*LOX*) is a key copper dependent amine oxidase enzyme that functions in the final steps of collagen and elastin biosynthesis (1, 2). Extracellularly, LOX catalyzes the oxidation reaction of lysine and hydroxylysine side chains located on the telopeptide regions of fibrillar procollagens to allysine and hydroxyallysine, respectively (3). These highly reactive aldehyde residues self-coalesce into normal immature and mature cross-links in collagen fibrils (4). From there, the collagen mineralizes and forms the fundamental structure of bone.

The biosynthesis of Lox has been explored using rat vascular smooth muscle cells by Trackman and others. Lox begins as a 46 kDa preproprotein consisting of three domains: an N-terminal signal peptide, a propeptide, and a catalytic domain (2, 3, 5). Inside the cell, the signal sequence is removed and the propeptide domain is N-glycosylated for travel through the Golgi, and is subsequently released outside the cell as an inactive protein (5). The 50 kDa pro-protein is cleaved yielding the active enzyme by BMP-1, and two other procollagen C-proteinases (6).

There are five isoforms of lysyl oxidase, including LOX and lysyl oxidase-like 1-4 (LOXL1-LOXL4). LOX and LOXL1-LOXL4 have a conserved C-terminal domain, but differ in that LOXL2-LOXL4 have four scavenger receptor cysteine rich domains; LOX and LOXL1 do not have such cysteine-rich domains. Additionally, more investigation has been done explaining the expanded role of these isoforms in cases of fibrosis, cancers, and diabetic complications (3), thus suggesting that LOX and its isoforms are not solely involved in bone development and maturation. Studies have shown that

LOXL1 has sex-specific bone abnormalities in *Loxl1* knockout mice (1, 7). Furthermore, LOX and its isoforms have a paradoxical role when it comes to their role in cancer (8-10). Some studies have shown that Lox plays a more tumor promoting role, while the Lox pro-peptide, cleaved off during biosynthesis, serves a protective role (10-12). However, it is widely considered that LOX is able to alter the tumor microenvironment, and is a key marker in cancer detection and a potential target in cancer therapy (8). In a recent study the mechanism by which LOXL2 promotes cancer progression and development was elucidated. The authors found tumor cell LOXL2 stimulates oral fibroblasts by oxidizing the PDGFR**β** receptor on oral fibroblasts, resulting in increased cell proliferation (13). Therefore, LOX and its isoforms have been shown to have a wide effect on bone and tumor development.

In a historical background, back in the days of Hippocrates, lysyl oxidase was beginning to show its role in bone development. After a string of neurological issues plaguing the animals and some people of his city, Hippocrates wrote that the constant between the two groups was the *Lathyrus* seeds they consumed (14). Later, the condition would be known as lathyrism. However, lathyrism occurs in two main varieties; neurolathyrism and osteolathyrism, both terms coined by Selye in 1957. One variant affects the neurological system primarily, the other, the skeleton. However, this was not an isolated incident. Many occurrences throughout the 15th and up until the early 20th centuries were described (14). All seemed to have a common theme: a time of either low crop yield and or famine, which led the community to supplement their food with the *Lathyrus* sweet pea (14). This was primarily due to its robust ability to grow in harsh

conditions, and its resistance to blight. Yet, when these seeds would be consumed, signs of muscle weakness and even paralysis of the lower extremities were found, and seemed to affect more males than females (14, 15). These effects were seen in many animals, including: birds, livestock, and horses (16). Aortic lesions were common in later experiments involving mice (17). Therefore, considerable amounts of research were conducted to find the answer to these disorders. More specifically, in 1955 a handful of researchers isolated the substance known as **β**, **γ** L-glutamylaminopropionitrile, which is metabolized to **β**-aminopropionitrile (BAPN) (14, 17). BAPN is the natural inhibitor of lysyl oxidase, and is widely used today in the study of lysyl oxidase and its role in bone development. Therefore, lathyrism was caused by the lysyl oxidase inhibitor, BAPN which is concentrated in the Lathyrus Sweet Pea species of plants. Thus, early evidence already pointed to the importance of lysyl oxidase activity to the structure and function of bone and other connective tissues.

The role LOX plays in the strength of bone cannot be understated. Such effects can be seen in diseases such as osteogenesis imperfecta, diabetes mellitus, chronic kidney disease, and osteoporosis (18, 19) . Bone structural changes leading to decreased integrity is heavily related to cross-linking mishaps as part of the disease process (18). Defects in the production or cross-linking of type 1 collagen shows significant bone strength reduction as well as changes in the turnover rate in patients with osteogenesis imperfecta (OI) (20). Microcracking seen in experimental animal models lead researchers to believe this is the mechanism for such an altered turnover. An increase in turnover is also seen in patients with Paget's Disease, of which there is significant

disorganization of the microarchitecture, leading to impaired strength as a result of altered C-telopeptide regions of type 1 collagen (19). McNerny and colleagues found a dose-dependent relationship between different subcutaneous concentrations of BAPN in a mouse model, which lead to decreased collagen cross-linking and decreased bone strength and fracture stiffness (21). In another recent study, Paschalis et. al. found decreased trabecular bone volume versus tissue ratio, decreased trabecular thickness, and altered collagen cross-linking in rats fed with a BAPN laced diet (22). Furthermore, they noted that bone mineral density distribution (BMDD) was not altered in the experimental rats (22). Lastly, in another BAPN lathyrism model, Oxlund and colleagues found rats treated with BAPN had a reduction of 45% in concentration of hydroxypyridinium crosslinks, a 31% decrease in bone stability toward acid attack, and significant reductions in breaking, bending stress, and elastic stiffness (23).

When it comes to bone development, there are two main classifications from which the skeleton is derived; that being the membranous and endochondral skeletal development (27). Both avenues rely on three main embryonic lineages: Neural crest cells, paraxial mesoderm cells, and lateral plate mesoderm cells (27). The key difference between the two routes is their method for how bone is produced. Membranous development uses osteoblasts developed from mesenchymal cells that begin to lay down the direct preliminary bone matrix, and endochondral first uses chondrocytes that produce cartilage which later ossifies into a bone network (27). Deposition is a result of cell condensation, a process that sees cells clustering together prior to the initiation of the organ development (28). Depending on the location of the bone, one will find the type of

development. Membranous developed bones are the head and collar bone structures, and endochondrally developed are bones of the axial skeleton and limbs (27).

Osteoblasts are the keystone for the development and production of bone and the extracellular environment bone is created. Osteoblast development begins inside the bone marrow, where mesenchymal stem cells (MSC) are induced to begin their differentiation into these bone producing cells. During the differentiation, proliferation of the MSC cells yields a committed osteoprogenitor to become an osteoblast, and another stem cell to carry on the undifferentiated lineage. Key transcriptional regulators of osteoblast differentiation are Runx2, Osterix, ATF4, and SATB2 (29). Once the osteoblast has developed, proteins such as type 1 collagen, osteocalcin (OCN), and osteopontin are secreted to begin formation of the bone tissue (30). Osteoblasts that do not continue laying down osteoid fall into one of two fates, apoptosis, or they become integrated into the bone as osteocytes (31). However, it is important to think of bone formation and maintenance as a coordinated system of bone-building osteoblasts and bone-destroying osteoclasts. It has been found that osteoclasts are regulated by estrogen to some degree, and postmenopausal women who have lowered serum estrogen show increased osteoclast activity (29). Such activity leads to the bone disorders so often affecting this sex-age group such as osteoarthritis and osteoporosis, indicating that estrogen could be providing a protective element. Thus, elucidating the mechanisms behind osteoblast development and cell cycle could answer questions regarding bone disorders in our aging population.

In order to knockout *Lox* in osteoblasts, we used the promoter of the osteoblast specific hormone, osteocalcin (*Ocn*) to drive Cre-Recombinase and produce the

osteoblast *Lox* knockout (12). The human osteocalcin gene is found on chromosome 1, 1q25-q31 (4). Osteocalcin, also known as gamma-carboxyglutamic acid protein, is expressed in the later stages of osteoblast development and once it has undergone splicing, it shows an affinity for bone and the extracellular matrix (13)(32). Moreover, OCN has been thought to play a larger role in the mineralization process instead of a role in matrix deposition (32). There are two forms of OCN, the uncarboxylated form and the carboxylated form. Uncarboxylated OCN has been shown to be involved in insulin regulation with pancreatic islet cells (24, 25), and uses the Gprc6a receptor to induce its effects (26). Meanwhile, the carboxylated form of OCN is believed to serve a direct mechanical role in the bone architecture via bonding with osteopontin and integration of this complex into the hydroxyapatite network (4).

In order to use the *Cre*-lox Recombinase system in our study, the design of the first floxed *Lox* mouse was done so using CRISPR-Cas9 technology. Since the 1980s, CRISPR-Cas9 (Clustered Regularly-Interspaced Short Palindromic Repeats)-Cas9 (Crisper associated protein 9) has been a key component of molecular genetics research. CRISPR is able to edit genomes, providing seemingly endless avenues of study for potential therapeutic remedies and pathologic inquiry. The method this nuclease employs is the use of a 20 nucleotide RNA (gRNA) which targets the specific region in a target DNA (33). CRISPR finds this region and makes a cut 3 base pairs upstream of a PAM (Protospacer Adjacent Motif) (33). With the DNA cleaved, the DNA of interest is now added, allowing for the pairing with the end cut location of the host DNA. Finally, the DNA strands are brought back together through NHEJ (Non-Homologous End Joining)

or by HDR (Homology Directed Repair) and subsequent integration into the host genome (33). In our lab, this was done using mouse embryos that were later implanted into female mice, thereby creating the proper genomic sequence for future mouse studies. Therefore, through CRISPR technology, our lab was able to produce the first *Lox*-floxed mouse; setting up what would be our experiment to knockout *Lox* in mouse osteoblasts.

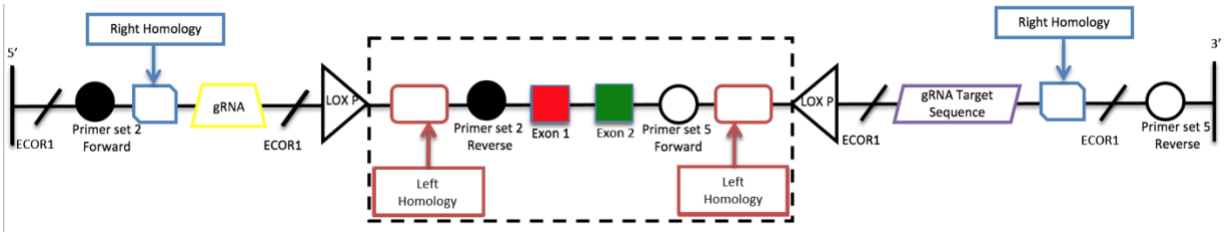

Figure 1: Graphic representation of the genome in a homozygous lox flox mouse is presented. This drawing is not to scale. Diagonal black lines represent ECOR1 restriction enzyme cutting sites. Black filled or hollow circles represent primer set 2 and 5 binding sites, respectively. The sequences for Primer set 2 and 5 are as follows: Primer set 2 forward: CTTGTGCTCCCTCTACTGGTG. Primer set 2 reverse: GATGCGCTGC GGAAGAAAAC. Primer set 5 forward: CGTTGCACAGGGAGAGTTAAG. Primer set 5 reverse: TAAAGTGCAAATTGGGCTGGT. Blue rectangles with angled corners represent the right homology. Yellow trapezoid represents the gRNA. Black triangles indicate loxp binding sites. Red smooth cornered rectangles depict left homology. The red box indicates exon 1, whereas the green box represents exon 2. The purple lined trapezoid shows the gRNA target sequence. Lastly, the dashed box surrounding the sequences flanked by the LOX P sites show what is being excised when a lox fl/fl mouse is crossed with a *Ocn-cre*$^{+/-}$ mouse, giving *Ocn-cre +/-, Lox* $^{fl/fl}$ *progeny.*

Analyzing phenotypic changes in the study mice will rely, in part on µCT imaging. µCT has been regarded as an optimal method for evaluation of mineralized structures (34). Furthermore, recent studies have shown soft tissue evaluation in vivo without the need of ex vivo sampling (35). The basics of µCT rely on the generation of

x-rays projected at multiple angles which pass through a series of initial collimators and filters prior to traversing through the sample itself (34). These x-rays are then picked up on a detector which integrates them into a 3D pixel known as a voxel. Voxels through computation algorithms are then organized into a 3D depiction of the scanned sample to be further investigated. The x-ray beam can be controlled at it's source by regulation of the voltage and current. Most studies agree that the voltage for scanning hard tissue to be set at 50-70 kV while current is best set between 115-150 μA (34, 35). Similarly, voxel size also plays a role in the depiction of the bone structure. Voxel sizing that is too large or too small in regards to the source of tissue being scanned may lead to underestimation or overestimation of key structures (36). For scanning of smaller animals' structures, such as mouse femurs, voxel size is recommended to be around 10 μm^3(34, 36). A detailed description of the scanning parameters for the samples in this study is presented in the Methods section.

Our hypothesis for the following experiment is the *Ocn-cre* +-, $Lox^{fl/fl}$ mice will have an altered bone phenotype in contrast to the *Ocn-cre*$^{-/-}$, *Lox*$^{fl/fl}$ controls through μCT and histological analysis. We believe a change in the skeletal phenotype may occur in later stages of the osteoblast development due to Ocn being expressed late in the sequence of gene expression changes as a function of osteoblast differentiation. Thus our working hypothesis is that Ocn-driven conditional deletion of Lox will lead to a significant phenotype in mice with nearly fully developed skeletons.

METHODS

Our group employed the Cre-*lox* recombinase system to knockout *Lox* in mouse osteoblasts using the osteocalcin promoter to drive cre recombinase. C57BL/6J male and female mice were selected and bred to achieve the breeding pair genotypes *Ocn-cre*$^{+/-}$, *Lox*$^{fl/-}$ and Lox$^{fl/fl}$. The progeny we chose for the experimental group were *Ocn-cre*$^{+/-}$, Lox$^{fl/fl}$, and the control group genotypes being *Ocn-cre*$^{-/-}$, *Lox*$^{fl/fl}$. We analyzed the differences between 13-week old male and female *Ocn-cre*$^{+/-}$, *Lox*$^{fl/fl}$ and *Ocn-cre*$^{-/-}$,*Lox*$^{fl/fl}$ using µCT analysis and histological analysis. Genotyping was confirmed for each mouse through genomic DNA isolation from tail samples; and subsequent PCR, EcoR1 restriction enzyme digestion, and gel electrophoresis was conducted. The primer sets of interest were the OCN-*cre* primer set, *Lox* primer set 2, and *Lox* primer set 5. Reactions from both primer set 2 and 5 were digested for 2 hours prior to gel electrophoresis using the restriction enzyme EcoR1; the *Ocn-cre* primer set needed no such digestion prior to the gel electrophoresis. 50µL of each sample was loaded into separate wells of a 1.5% agarose gel with 5 µL of ethidium bromide and 1x Tris/Acetate/EDTA (TAE) buffer. 110 Volts was then applied for approximately 1 hour and 15 minutes. The gel was then placed over an ultraviolet light and photographed and analyzed for the DNA of interest.

µCT analysis was carried out at the Center for Skeletal Research Imaging and Biomechanical Testing Core under the grant NIH P30 AR070542. 6 Female *Ocn-cre*$^{-/-}$, *Lox*$^{fl/fl}$, 6 Female *Ocn-cre*$^{+/-}$, *Lox*$^{fl/fl}$ 6 Male *Ocn-cre*$^{-/-}$, *Lox*$^{fl/fl}$, and 6 Male *Ocn-cre*$^{+/-}$, *Lox*$^{fl/fl}$ were submitted for analysis. All mice were 13 weeks of age.

The following text was provided by Dr. Mary Bouxsein's laboratory, which carried out the µCT analyses. "A high-resolution desktop micro-tomographic imaging system (µCT40, Scanco Medical AG, Brüttisellen, Switzerland) was used to assess trabecular bone microarchitecture in the distal femoral metaphysis, whereas cortical bone morphology was assessed at the femoral midshaft. Scans were acquired using a 10 µm3 isotropic voxel size, 70 kVP, 114 mAs, 200 ms integration time, and were subjected to Gaussian filtration and segmentation. Image acquisition and analysis protocols adhered to the JBMR guidelines (1) . For the distal femur, transverse CT slices were evaluated in an 1500 µm (150 slices) region beginning 1700 µm above the peak of the growth plate and extending distally to 200 µm above the top of the growth plate. The trabecular bone region was identified by semi-manually tracing the region of interest with the assistance of an auto-thresholding software algorithm. An adaptive-iterative algorithm(2-4) was used to select a mineral density threshold of 350 mgHA/cm3 to segment trabecular bone from soft tissue. Morphometric variables were computed from the binarized images using direct, 3D techniques that do not rely on any prior assumptions about the underlying structure(5-7). For trabecular bone regions, we assessed the bone volume fraction (BV/TV, %), trabecular thickness (Tb.Th, mm), trabecular number (Tb.N, mm^{-1}), trabecular separation (Tb.Sp, mm), connectivity density (ConnD, $1/mm^3$), and structure model index (SMI), a parameter that describes the plate-vsrodlike nature of the architecture. Higher values of SMI indicate rod-like structures, whereas lower values characterize plate-like ones" (37).

"To assess cortical bone parameters, 50 transverse μCT slices were obtained at the femoral mid-diaphysis using a 10 μm isotropic voxel size. The ROI included the entire outer most edge of the cortex. Images were subjected to Gaussian filtration and segmented using a fixed threshold of 700 mgHA/cm3. The following variables were computed: total cross-sectional area (bone + medullary area) (Tt.Ar, mm2), cortical bone area (Ct.Ar, mm2), medullary area (Ma.Ar, mm2), bone area fraction (Ct.Ar/Tt.Ar, %), cortical tissue mineral density (Ct.TMD, mgHA/cm3), cortical thickness (Ct.Th, mm), cortical porosity (%), as well as maximum, minimum and polar moments of inertia (Imax, Imin, and J, mm4), which describe the shape/distribution of cortical bone (larger values indicate a higher bending strength)" (37).

"Statistics: Unpaired t-tests were performed to compare the trabecular and cortical parameters of OCN-Cre- and OCN-Cre+ mice within each gender. P-values and means ± SD are reported" (37).

RESULTS

μCT analysis of the female 13-week old *Ocn-cre*$^{+/-}$, *Lox*$^{fl/fl}$ mice showed statistically significant reduction in Bone Volume/Total Volume (BV/TV) ($P<0.003$), Connective Tissue Density (ConnD) ($P<0.012$), Bone Mineral Density (BMD) ($P<0.001$), and Structural Model Index (SMI) ($P<0.004$). Male 13-week old *Ocn-cre*$^{+/-}$, Lox$^{fl/fl}$ mice showed no statistically significant differences in any parameters analyzed.

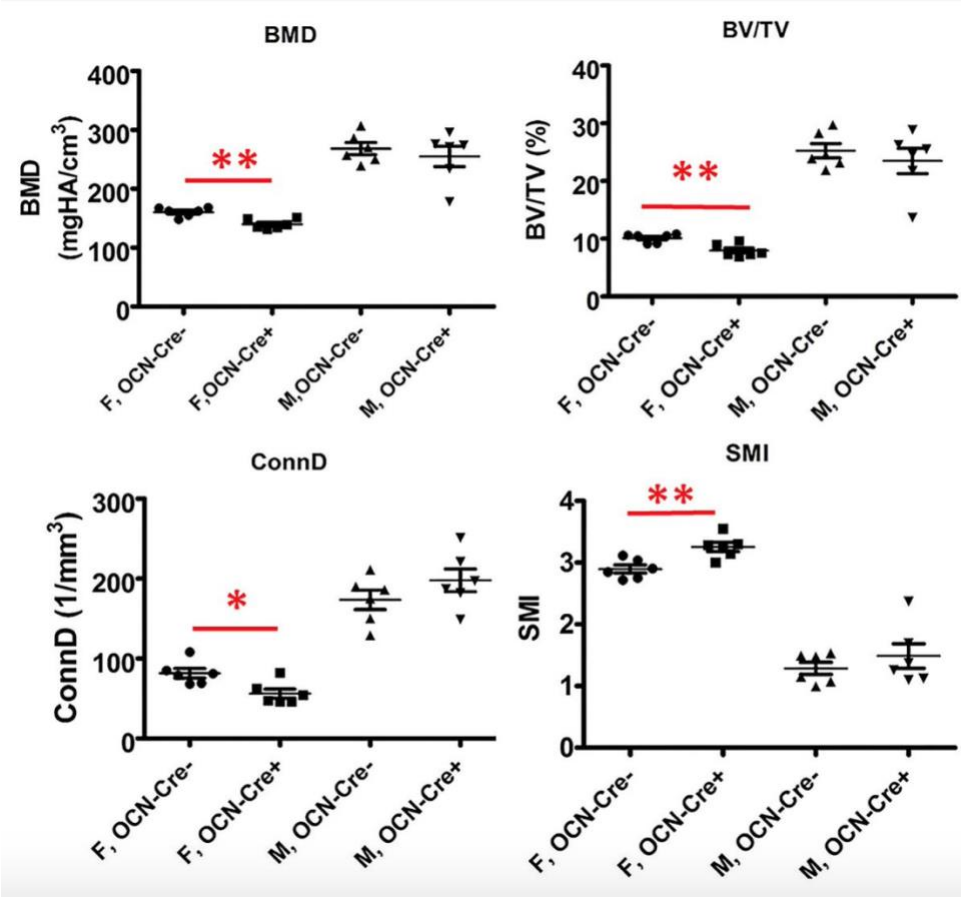

Figure 2: Graphical representation of the micro-CT values of *Lox*$^{fl/fl}$ mice either expressing Ocn-*cre*+, or not (OCN-*cre*-, control). (From left to right, top to bottom) Bone Mineral Density (BMD), Bone Volume/Tidal Volume (BV/TV), Connective tissue density (ConnD), Structural Model Index (SMI).

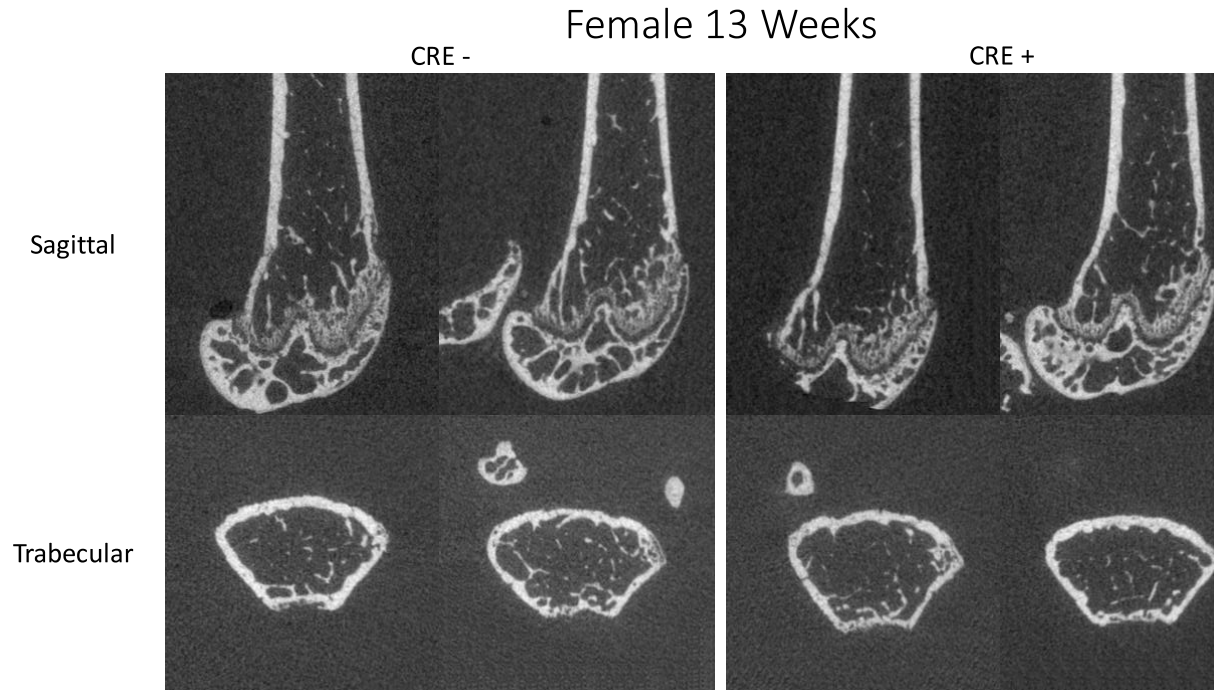

Figure 3: µCT images from 13-week old female *Ocn-cre+/-*, *Lox*$^{fl/fl}$ and *Ocn-cre*$^{-/-}$, *Lox*$^{fl/fl}$ mice showing the femoral head and mid-diaphysis regions.

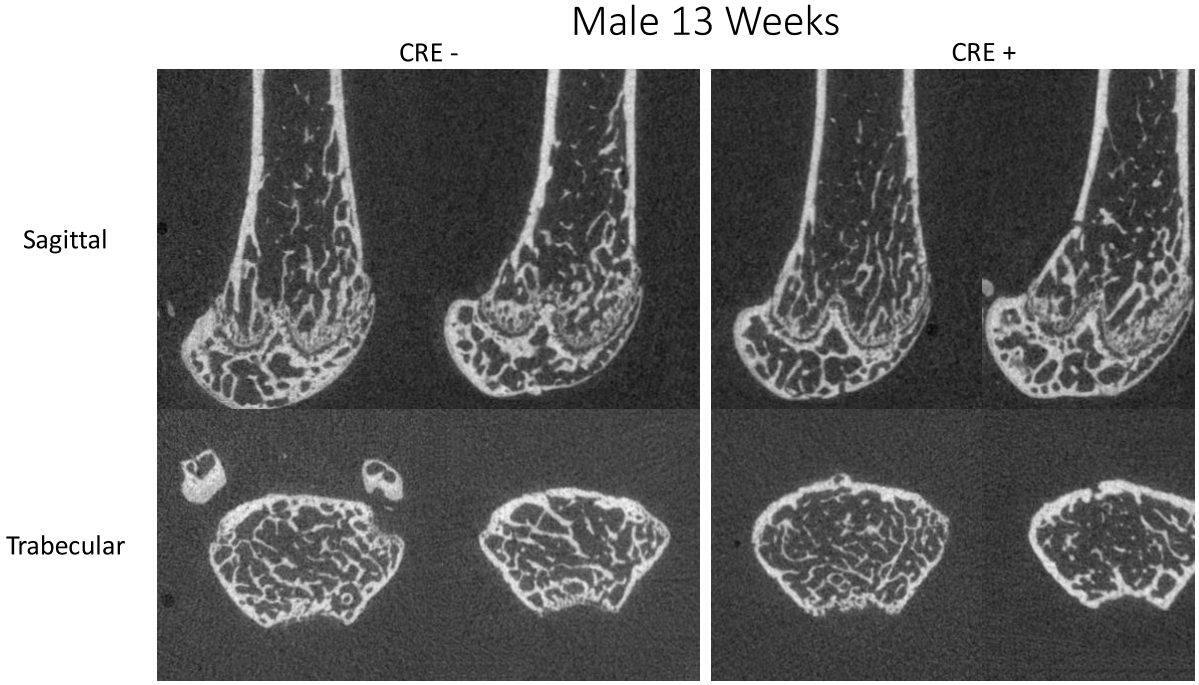

Figure 4: µCT images from 13-week old male *Ocn-cre*$^{+/-}$, *Lox*$^{fl/fl}$ and *Ocn-cre*$^{-/-}$, *Lox*$^{fl/fl}$ mice showing the femoral head and mid-diaphysis regions.

Histology: H&E staining of tibia sections showed a statistically significant decreases in the number of chondrocytes per column in the *cre*+ female and male mice. The largest differences in number of chondrocytes per column were found in female *cre*+ mice.

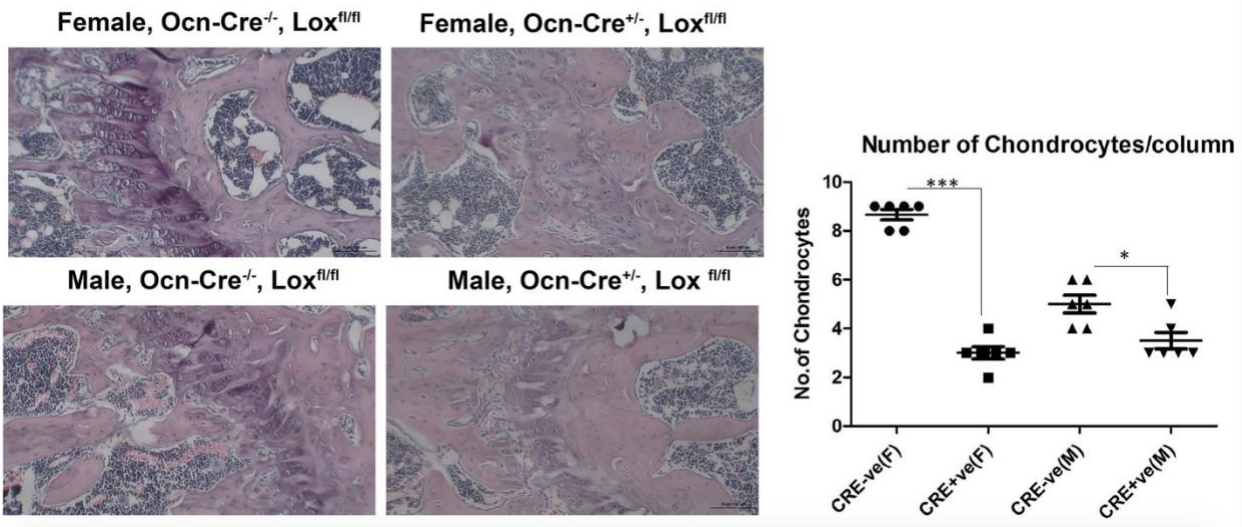

Figure 5: H&E stained sections of mice presented. Histological analysis was performed by Vrinda Dambal. The graph to the right side of the figure shows the number of chondrocytes per column observed in the histological sections.

DISCUSSION

A more significant alteration in bone parameters was expected in the osteocalcin promoter-driven osteoblast knockout model. Yet, we believe this may be a result of Ocns rather late expression in osteoblasts (32). With this in mind, our rationale is that the role Lox plays in collagen crosslinking may have already be largely completed by the 13-week time mark, or by the time osteoblasts enter the late phases of differentiation. Thus,

this may lead to a reduced, yet still significant change in BMD, BV/TV, ConnD, and SMI values at least in female mice at this age. Other studies have shown Lox family and elastin gene (*Eln*) activity decrease with age in female mice (38). Perhaps further time course studies investigating this aspect should be the next steps with this model. An alternative test to this hypothesis is to knockout Lox using an earlier-expressed osteoblast promoter, such as provided by the Col2.3-cre mouse.

The organization of chondrocytes in the growth plate of femurs in both females and males were decreased. Females showed a more significant decrease as compared to the males. These results are similar to those found by Alsofi et. al, who looked at sex-linked phenotype of Loxl1 global knockout mice (1). In their study, 13-week old females also showed disrupted chondrocyte organization compared to male counterparts, as well as statistically significant decreases in BV/TV and ConnD in the distal metaphysis. It is known that Lox expression is needed for C3H10T1/2 cell line differentiation into chondrocytes (3). Therefore, a possible reason for a decrease in chondrocytes seen may be due to secondary effects of Lox knockout in osteoblasts. Additionally, another possible explanation for such a change in the number of chondrocytes per column in the females as compared to the males may be due to estrogen's effect on LOX. Lee et. al. found LOX expression was reduced when estrogen was added to an experimental ligament model, which also revealed decreased strength and function (7). Thus, in addition to the secondary effects of the *Lox* knockout, estrogen may have further reduced Lox's chondrocyte differentiation signaling leading to decreased chondrocytes per column compared to males. In contrast, Lox expression has been shown to be increased

by estrogen and decreased by progesterone in mouse uterus, while combined estrogen and progesterone delivery showed no effect (39). Elucidation of this interplay between Lox regulation via sex hormones needs analysis.

CONCLUSION

Overall, the difference in phenotype, albeit not as large as we had hoped, gives further insight to the role Lox plays in the overall development and homeostasis of bone. Clear evidence has existed for some time showing strength and microarchitectural changes occurring when LOX activity or other defects in type 1 collagen exist. Clinical implications of such defects are found in the diseases mentioned above, and their impact on patients is significant. Further investigation into osteoblast specific *Lox* knockout should be conducted.

REFERENCES

1. Alsofi, L., Daley, E., Hornstra, I., Morgan, E.F., Mason, Z.D., Acevedo, J.F., Word, R.A., Gerstenfeld, L.C., and Trackman, P.C. (2016) Sex-Linked Skeletal Phenotype of Lysyl Oxidase Like-1 Mutant Mice. *Calcified Tissue International.* 172-185

2. Tang, C., and Klinman, J.P. (2001) The catalytic function of bovine lysyl oxidase in the absence of copper. *Journal of Biological Chemistry.* **33,**

3. Trackman, P.C. (2016) Enzymatic and non-enzymatic functions of the lysyl oxidase family in bone. *Matrix Biology.* **52,** 7-18

4. Zoch, M.L., Clemens, T.L., and Riddle, R.C. (2015) New insights into the biology of osteocalcin. *Bone.* **82,** 42-49

5. Trackman, P.C., Bedell-Hogan, D., Tang, J., and Kagan, H.M. (1992) Post-translational Glycosylationand Proteolytic Processingof a Lysyl Oxidase Precursor*__267,__

6. Kagan, H.M., and Li, W. (2003) Lysyl oxidase: Properties, specificity, and biological roles inside and outside of the cell. *Journal of cellular biochemistry.* **88,** 660-672

7. Lee, C.A., Lee-Barthel, A., Marquino, L., Sandoval, N., Marcotte, G.R., and Baar, K. (2015) Estrogen inhibits lysyl oxidase and decreases mechanical function in engineered ligaments. *Journal of applied physiology (Bethesda, Md. : 1985).* **118,** 1250-1257

8. Wang, T., Hsia, S., and Shieh, T. (2016) Lysyl Oxidase and the Tumor Microenvironment. *International journal of molecular sciences.* **18,** 62

9. Nilsson, M., Adamo, H., Bergh, A., and Halin Bergström, S. (2016) Inhibition of Lysyl Oxidase and Lysyl Oxidase-Like Enzymes Has Tumour-Promoting and Tumour-Suppressing Roles in Experimental Prostate Cancer. *Scientific reports.* **6,** 19608

10. Ozdener, G.B., Bais, M.V., and Trackman, P.C. (2016) Determination of cell uptake pathways for tumor inhibitor lysyl oxidase propeptide. *Molecular Oncology.* **10,** 1-23

11. Zheng, Y., Wang, X., Wang, H., Yan, W., Zhang, Q., and Chang, X. (2014) Expression of the lysyl oxidase propeptide in hepatocellular carcinoma and its clinical relevance. *Oncology Reports.* **31,** 1669-1676

12. Bias, M.V., Nugent, M.A., Stephens, D.N., Sume, S.S., Kirsch, K.H., Sonenshein, G.E., and Trackman, P.C. (2012) Recombinant Lysyl Oxidase Propeptide Protein Inhibits

Growth and Promotes Apoptosis of Pre-Existing Murine Breast Cancer Xenografts. *PLoS One.* **7,** e31188

13. Mahjour, F., Dambal, V., Shrestha, N., Singh, V., Noonan, V., Kantarci, A., and Trackman, P.C. (2019) Mechanism for oral tumor cell lysyl oxidase like-2 in cancer development: synergy with PDGF-AB. . *Oncogenesis.* **8,**

14. Barrow, M.V., Simpson, C.F., and Miller, E.J. (1974) Lathyrism: A Review. *The Quarterly Review of Biology.* **49,** 101-128

15. Rowe, D.W., McGoodwin, E.B., Martin, G.R., Sussman, M.D., Grahn, D., Faris, B., and Franzblau, C. (1974) A Sex-Linked Defect in the Cross-Linking of Collagen and Elastin Associated with the Mottled Locus in Mice. *Journal of Experimental Medicine.* **139,** 180-192

16. Manna, P.K., Mohanta, G.P., Villiappan, K., and Manavalan, R. (1999) Lathyrus and Lathyrism: A Review. *International Journal of Food Properties.* **2,** 197-203

17. McCallum, H.M. (1958) Lathyrism in Mice. *Nature.* 1169-1170

18. Saito, M., and Marumo, K. (2015) Effects of Collagen Crosslinking on Bone Material Properties in Health and Disease. *Calcified Tissue International.* **97,** 242-261

19. Garnero, P. (2015) The Role of Collagen Organization on the Properties of Bone. *Calcified Tissue International.* **97,** 229-240

20. Alford, A.I., Kozloff, K.M., and Hankenson, K.D. (2015) Extracellular matrix networks in bone remodeling. *The International Journal of Biochemistry & Cell Biology.* 20-31

21. McNerny, E.M., Gong, B., Morris, M.D., and Kohn, D.H. (2014) Bone Fracture Toughness and Strength Correlate With Collagen Cross-Link Maturity in a Dose-Controlled Lathyrism Mouse Model. *Journal of Bone and Mineral Research.* **30,** 455-464

22. Paschalis, E.P., Tatakis, D.N., Robins, S., Fratzl, P., Manjubala, I., Zoehrer, R., Gamsjaeger, S., Buchinger, B., Roschger, A., Phipps, R., Boskey, A.L., Dall'Ara, E., Varga, P., Zysset, P., Klaushofer, K., and Roschger, P. (2011) Lathyrism-induced alterations in collagen cross-links influence the mechanical properties of bone material without affecting the mineral. *Bone.* **49,** 1232-1241

23. Oxlund, H., Barckman, M., Ortoft, G., and Andreassen, T.T. (1995) Reduced Concentrations of Collagen Cross-links are Associated with Reduced Strength of Bone. *Bone.* **17,** 365S-371S

24. Lee, N.K., Sowa, H., Hinoi, E., Ferron, M., Ahn, J.D., Confavreux, C., Dacquin, R., Mee, P.J., McKee, M.D., Jung, D.Y., Zhang, Z., Kim, J.K., Mauvais-Jarvis, F., Ducy, P., and Karsenty, G. (2007) Endocrine Regulation of Energy Metabolism by the Skeleton. *Cell.* **130,** 456-469

25. Jing-Wen Wang, Qing-Ya Tang, Hui-Juan Ruan, and Wei Cai (2014) Relation Between Serum Osteocalcin Levels and Body Composition in Obese Children. *Journal of Pediatric Gastroenterology and Nutrition.* **58,** 729-732

26. Pi, M., Wu, Y., and Quarles, L.D. (2011) GPRC6A mediates responses to osteocalcin in β -cells in vitro and pancreas in vivo. *Journal of Bone and Mineral Research.* **26,** 1680-1683

27. Horton, W.A. (2003) Skeletal Development: insights from targeting the mouse genome. *The Lancet.* **362,** 560-569

28. Hall, B.K., and Miyake, T. (2000) All for one and one for all: condensations and the initiation of skeletal development. *BioEssays.* **22,** 138-147

29. Huang, W., Yang, S., Shao, J., and Li, Y. (2007) Signaling and transcriptional regulation in osteoblast commitment and differentiation. *Frontiers in Bioscience.* 3068-3092

30. Blair, H.C., Larrouture, Q.C., Li, Y., Lin, H., Beer-Stoltz, D., Liu, L., Tuan, R.S., Robinson, L.J., Schlesinger, P.H., and Nelson, D.J. (2017) Osteoblast Differentiation and Bone Matrix Formation In Vivo and In Vitro. *Tissue Engineering Part B: Reviews.* **23,** 268-280

31. Stein, G.S., Lian, J.B., Stein, J.L., Van Wijnen, A.J., and Montecino, M. (1996) Transcriptional Control of Osteoblast Growth and Differentiation. *Physiological Reviews.* **76,** 593-629

32. Lian, J.B., Stein, G.S., Stein, J.L., and van Wijnen, A.J. (1998) Osteocalcin Gene Promoter: Unlocking the Secrets for Regulation of Osteoblast Growth and Differentiation. *Journal of Cellular Biochemistry Supplements.* **30,** 62-72

33. Zhang, J., Adikaram, P., Pandey, M., Genis, A., and Simonds, W.F. (2016) Optimization of genome editing through CRISPR-Cas9 engineering. *Bioengineered.* **7,** 166-174

34. Bouxsein, M., Boyd, S., Christiansen, B., Guldberg, R.E., Jepsen, K.J., and Muller, R. (2010) Guidelines for Assessment of Bone Microstructure in Rodents Using Micro-Computed Tomography. *Journal of Bone and Mineral Research.* **25,** 1468-1486

35. Campbell, G.M., and Sophocleous, A. (2014) Quantitative analysis of bone and soft tissue by micro-computed tomography: applications to ex vivo and in vivo studies. *BoneKEy Reports.*

36. Tjong, W., Kazakia, G.J., Burghardt, A.J., and Majumdar, S. (2012) The effect of voxel size on high-resolution peripheral computed tomography measurements of trabecular and cortical bone microstructure. . *Medical Physics.* **39,** 1893-1903

37. Bruce, M. (2019) Center for Skeletal Research Imaging and Biomechanical Testing Core NIH P30 AR070542

38. Jiang, Y., Zong, W., Luan, H., Liu, J., Zhang, A., Li, X., Liu, S., Zhang, S., and Gao, J. (2014) Decreased expression of elastin and lysyl oxidase family genes in urogenital tissues of aging mice. *Journal of Obstetrics and Gynaecology Research.* **40,** 1998-2004

39. Li, S., Yan, J., Song, Z., Liu, Y., Song, M., Qin, J., Yang, Z., and Liang, X. (2017) Molecular characterization of lysyl oxidase-mediated extracellular matrix remodeling during mouse decidualization. *FEBS Letters.* **591,** 1394-1407

CURRICULUM VITAE